Prediction of the tissue-specificity of selective estrogen receptor modulators by using a single biochemical method

Susie Y. Dai*, Michael J. Chalmers*, John Bruning†, Kelli S. Bramlett‡§, Harold E. Osborne‡, Chahrzad Montrose-Rafizadeh‡, Robert J. Barr‡, Yong Wang‡, Minmin Wang‡, Thomas P. Burris‡¶, Jeffrey A. Dodge‡, and Patrick R. Griffin*‖**

Departments of *Molecular Therapeutics and †Cancer Biology and ‖The Scripps Research Molecular Screening Center (SRMSC),The Scripps Research Institute, Jupiter, FL 33458; and ‡Lilly Research Laboratories, Eli Lilly and Company, Indianapolis, IN 46285

Edited by John A. Katzenellenbogen, University of Illinois at Urbana–Champaign, Urbana, IL, and accepted by the Editorial Board March 20, 2008 (received for review November 14, 2007)

Here, we demonstrate that a single biochemical assay is able to predict the tissue-selective pharmacology of an array of selective estrogen receptor modulators (SERMs). We describe an approach to classify estrogen receptor (ER) modulators based on dynamics of the receptor-ligand complex as probed with hydrogen/deuterium exchange (HDX) mass spectrometry. Differential HDX mapping coupled with cluster and discriminate analysis effectively predicted tissue-selective function in most, but not all, cases tested. We demonstrate that analysis of dynamics of the receptor–ligand complex facilitates binning of ER modulators into distinct groups based on structural dynamics. Importantly, we were able to differentiate small structural changes within ER ligands of the same chemotype. In addition, HDX revealed differentially stabilized regions within the ligand-binding pocket that may contribute to the different pharmacology phenotypes of the compounds independent of helix 12 positioning. In summary, HDX provides a sensitive and rapid approach to classify modulators of the estrogen receptor that correlates with their pharmacological profile.

discriminate analysis | hydrogen/deuterium exchange | mass spectrometry

The estrogen receptors (ERα and ERβ) are important transcriptional regulators that mediate a number of fundamental processes including regulation of the reproductive system and the maintenance of skeletal and cardiovascular tone. As such, these receptors are the molecular targets of drugs used to treat diseases such as breast cancer and osteoporosis. Both beneficial and detrimental effects of ER ligands have been demonstrated in target tissues, thus tissue-selective ER ligands have been developed and are termed selective estrogen receptor modulators (SERMs). Traditional drug discovery programs for ER modulators most often involve the use of a receptor-binding assay as a primary screen to identify high-affinity ligands, followed by the use of *in vitro* cell-based assays to determine the functional activity of a given ligand (1). Compounds with the desired intrinsic properties for affinity and selective functional response are then evaluated for *in vivo* efficacy in animal models of the targeted disease. Although this drug-discovery paradigm has been used successfully to identify most of the clinically-relevant SERMs discovered to date, the ability of *in vitro* biochemical and cell-based functional assays to translate to *in vivo* tissue selectivity has been limited. Cofactor recruitment assays have proven to be a useful tool to detect ligand-induced conformational changes for many nuclear receptors but can be less effective for profiling SERMs because the key coactivator interaction surface (AF-2) has been blocked by the ligand-induced repositioning of helix 12.

Classical approaches for structural analysis of receptor–ligand interaction involve the use of x-ray crystallography or NMR spectroscopy. The importance of studying changes to protein dynamics during ER modulation has been demonstrated by Tamrazi *et al.* (2). In a series of experiments, site-specific fluorescence labeling was used to probe receptor–ligand and receptor–coactivator interactions (2–4). Although it is a powerful technique, this approach has been limited to the measurement of the dynamics of regions around cysteine 417 and cysteine 530 (located near the C terminus of helix 11). Recently, hydrogen/deuterium exchange (HDX) coupled with proteolysis and mass spectrometry has evolved as a powerful method for rapid characterization of protein–protein and protein–ligand interactions (5–13). Briefly, the local environment of backbone amide hydrogens can be probed by measuring their rates of exchange with deuterium. The hydrogen/deuterium (H/D) exchange kinetics of amide protons vary as a function of hydrogen bonding and, to a lesser degree, are influenced by solvent accessibility (14). Mass spectrometry (MS) is ideally suited for HDX measurement because the technology provides high mass accuracy, high sensitivity, and is amenable to a high degree of automation. Importantly HDX MS allows for measurement of the majority of the residues within the target protein, a key advantage over the site-specific florescence labeling approach.

It has been demonstrated that ligand interactions with nuclear receptors alter the exchange kinetics of regions of the ligand-binding domain (LBD) directly involved in ligand binding, and in distal regions of the receptor that could not be predicted from cocrystal structures (13, 15). Here, we have applied HDX to study interactions of a collection of well characterized ER modulators. In addition, we have integrated statistical modeling with HDX analysis to classify ER modulators based on the peptide HDX signatures. We first applied HDX analysis to a series of known ER ligands with established tissue-selective pharmacological profiles by measuring the perturbations in hydrogen exchange of the ERαLBD on ligand binding. These ligands were then classified based on cluster analysis of their respective HDX peptide signatures. In the second step, we evaluated ER ligands within the same structural chemotype (benzothiophene) that contained subtle molecular differences. For the

Author contributions: S.Y.D., M.J.C., T.P.B., J.A.D., and P.R.G. designed research; S.Y.D., M.J.C., K.S.B., H.E.O., C.M.-R., R.J.B., Y.W., and M.W. performed research; J.B., K.S.B., H.E.O., R.J.B., Y.W., and M.W. contributed new reagents/analytic tools; S.Y.D., M.J.C., H.E.O., C.M.-R., Y.W., M.W., T.P.B., J.A.D., and P.R.G. analyzed data; and S.Y.D., M.J.C., T.P.B., J.A.D., and P.R.G. wrote the paper.

The authors declare no conflict of interest.

This article is a PNAS Direct Submission. J.A.K. is a guest editor invited by the Editorial Board.

Data deposition: The atomic coordinates have been deposited in the Protein Data Bank, www.pdb.org (PDB ID codes 2R6W and 2R6Y).

§Present address: Research and Development, Ambion, Inc., Austin, TX 78744.

¶Present address: Nuclear Receptor Biology Laboratory, Pennington Biomedical Research Center, Louisiana State University, Baton Rouge, LA 70808.

**To whom correspondence should be addressed at: The Scripps Research Institute, Scripps Florida, 5353 Parkside Drive, Jupiter, FL 33458. E-mail: pgriffin@scripps.edu.

This article contains supporting information online at www.pnas.org/cgi/content/full/0710802105/DCSupplemental.

Table 1. Activity of ER ligands

	Receptor affinity	ER-dependent cell assays				
Compound	K_i α, nM	MCF-7 (IC_{50}), nM	Ishikawa (IC_{50}), nM	Inhibition, %	Relative (EC_{50}), nM	Stimulation, %
4-hydroxytamoxifen	0.20 (0.17, $n = 4$)	0.63 (0.06, $n = 2$)	340.95 (706, $n = 295$)	55.8 (20.8, $n = 417$)	2.45 (6.6, $n = 404$)	131.3 (33.3, $n = 407$)
Lasofoxifene	0.34 (0.18, $n = 5$)	0.68 (0.01, $n = 2$)	6.97 (1.9, $n = 6$)	87.5 (8.5, $n = 6$)	0.22 (0.08, $n = 6$)	65.96 (17.5, $n = 6$)
LY165176	0.21 (0.08, $n = 6$)	6.1 ($n = 1$)	233.6 (123.5, $n = 2$)	61.5 (6.3, $n = 2$)	0.28 (0.25, $n = 2$)	128.7 (48.6, $n = 2$)
LY156681	0.44 (0.05, $n = 3$)	2.89 (1.7, $n = 3$)	NA	33.85 (3.5, $n = 4$)	4.67 (0.89, $n = 4$)	164.4 (30, $n = 4$)
Raloxifene (38)	0.37 (0.09, $n = 3$)	0.37 (0.03, $n = 2$)	4.32 (1.69, $n = 8$)	96.8 (7.0, $n = 8$)	NA	28.6 (8.5, $n = 8$)
Bazedoxifene	0.65 (0.17, $n = 3$)	0.47 ($n = 1$)	3.6 (1.8, $n = 274$)	99.1 (8.7, $n = 276$)	NA	7.6 (8.8, $n = 267$)
LY117018	0.32 (0.07, $n = 3$)	1.05 (0.55, $n = 34$)	3.42 (0.25, $n = 2$)	83.3 (2.1, $n = 2$)	0.39 (0.19, $n = 2$)	37.2 (17.6, $n = 2$)
Estradiol	0.16 (0.07, $n = 380$)	NA	NA	NA	0.81 (1.13, $n = 383$)	581.2 (273, $n = 383$)
DES	0.09 (0.05, $n = 3$)	NA	NA	NA	0.11 (0.01, $n = 2$)	410.7 (136.4, $n = 2$)
LY88074	0.67 (0.25, $n = 3$)	NA	NA	20.1 (7.4, $n = 2$)	105.7 (40.2, $n = 2$)	179.8 (34.5, $n = 2$)
ICI182780	3.0 (0.23, $n = 4$)	0.29 (0.20, $n = 3$)	0.58 (0.5, $n = 383$)	101.18 (7.06, $n = 386$)	NA	7.8 (10.8, $n = 375$)

MCF-7 values are half-maximal inhibition concentrations (nM) that block stimulation by 10 pM estradiol. Ishikawa agonism is the percentage increase in alkaline phosphatase compared with tamoxifen, whereas Ishikawa antagonism is the efficacy (%) of blocking 2 nM estradiol response, and the IC_{50} values are the compound concentration needed to block 50% of this estradiol stimulation. The numbers in parentheses are the SDs. Values without SD were run once.

subsequent statistical analysis, the peptide HDX signatures were treated as independent variables and the ER ligands treated as dependent variables. Results presented here demonstrate that HDX signatures provide a rapid and robust method to classify ER modulators. Cluster analysis of such signatures correctly assigned six of seven known estrogen modulators to functional classes, but incorrectly assigned the pure antagonist ICI 182780 to the estrogen agonist-like functional class. Similar HDX pattern-discriminant analysis allowed correct functional assignment of three of four benzothiophene-based unknowns into their biological phenotypes. As such, HDX is potentially useful for screening compound libraries and predicting ligand functional activity, thereby providing a predictive screen for novel SERMs.

Results

Pharmacological Properties of ER Modulators. A small collection of chemical compounds representing important ER ligand pharmacological phenotypes were characterized with a number of *in vitro* assays. These ligands included: 17β-estradiol (E2), the natural ER agonist; diethylstilbestrol (DES), a synthetic ER agonist; ICI 182780, an ER antagonist; and several SERMs with varying agonism/antagonism depending on tissue type (i.e., 4-hydroxytamoxifen and raloxifene). A series of estrogen-dependent *in vitro* assays were used to assess all ligands' affinity to ERα and ligand tissue-selective effects in breast and uterine tissues [see Table 1 and supporting information (SI) Text and Figs. S1–S4]. All compounds were found to have high affinity for ER with binding constants of <10 nM. In MCF-7 breast cancer cells, the SERMs 4-hydroxytamoxifen, lasofoxifene, raloxifene, and bazedoxifene were potent inhibitors of estradiol-stimulated proliferation as was ICI 182780. The effects on uterine tissue were assessed in human endometrial cells (Ishikawa) in the presence (antagonism) and absence (agonism) of E2. In agonist mode, 4-hydroxytamoxifen stimulates alkaline phosphatase activity 131% of control, with an EC_{50} of 2.5 nM (16). The agonist activities of lasofoxifene (66%), LY165176 (129%), and LY156681 (164%) were similar to that of 4-hydroxytamoxifen, whereas raloxifene (29%), LY117018 (37%), bazedoxifene (8%), and ICI 182780 (8%) were less agonistic than 4-hydroxytamoxifen.

HDX Analysis of ER Modulators. Comprehensive HDX analysis was performed with each ER–ligand complex, including all of the aforementioned ligands, and the results are summarized in Table 2. The values in Table 2 represent the average difference in deuterium incorporation percentages for each of the five on-exchange time points (see *Methods*) when comparing *apo* ERαLBD to the ligand-bound receptor LBD. Exchange kinetics for 28 different regions of the receptor LBD were measured and Fig. S5 shows the underlying percent deuterium (%D) vs. log time plots for three peptides representing two ER–ligand complexes (ER/E2 and ER/4-hydroxytamoxifen). These deuterium build-up curves were typical of all peptides measured in this study. The peptides showed differential HDX protection in a ligand-dependent and region-specific manner (a specific region within the binding pocket of the receptor). For example, the β-sheet1/β-sheet2 region (amino acids 403–410) was one region that demonstrated the most statistically significant ($P < 0.001$) differential HDX (i.e., ≈20% protection to exchange for 4-hydroxytamoxifen) depending on the ligand. Other regions of the binding pocket, such as helix 12, have no observable protection to exchange on binding all ligands studied, an interesting observation that we address in *Discussion*. The data in Table 2 indicate that agonists afford less stabilization or protection of exchange on binding receptor compared with receptor interaction with SERMs. Interestingly, the pure antagonist ICI 182780 also shows a similar HDX profile to that of agonists, which provides minimal stabilization of exchange on the receptor.

Statistical Analysis of HDX Signatures. We initially studied perturbations in HDX of the ERαLBD on binding of a series of known ER modulators that represented a diverse spectrum of chemical scaffolds and tissue-selective pharmacology. This included the agonists 17β-estradiol (E2) and DES, the pure antagonist ICI 182780 and the SERMs 4-hydroxytamoxifen [the active metabolite of tamoxifen (17)], raloxifene, lasofoxifene, and bazedoxifene

Table 2. Average differences in deuteration levels of *apo* ERαLBD in the presence of different ligands

Structure	AA #	End	Estradiol	4-hydroxy-tamoxifen	Raloxifene	DES	ICI	Lasodoxifene	Bazedoxifene	88074	156681	165176	117018
H2#	311	319	-4%	-8%	-6%	-3%	-5%	-9%	-7%	-3%	-6%	-8%	-5%
H2#	311	319	-3%	-7%	-6%	-2%	-5%	-8%	-8%	-3%	-6%	-9%	-5%
LOOP#	320	327	-7%	-16%	-11%	-6%	-3%	-16%	-11%	-6%	-11%	-14%	-10%
LOOP#	320	327	-4%	-13%	-10%	-3%	-3%	-13%	-7%	-5%	-7%	-10%	-8%
LOOP	328	339	-2%	-6%	-3%	-2%	-3%	-4%	-4%	-2%	-3%	-4%	-3%
LOOP	328	342	-4%	-7%	-4%	-4%	-4%	-5%	-6%	-3%	-4%	-9%	-5%
LOOP	328	343	-2%	-5%	-3%	-2%	-3%	-4%	-3%	-1%	-2%	-6%	-4%
H3#	343	349	-5%	-10%	-8%	-6%	-6%	-11%	-9%	-4%	-7%	-10%	-6%
H3#	343	349	-4%	-9%	-7%	-5%	-4%	-8%	-6%	-5%	-7%	-10%	-6%
H3	351	360	-3%	-13%	-8%	-3%	-5%	-10%	-11%	-4%	-6%	-12%	-9%
H5	371	380	-1%	-2%	-1%	0%	-2%	-3%	-1%	-1%	-2%	-4%	-1%
H5	373	380	-1%	-2%	-2%	0%	-1%	-3%	-2%	-1%	-2%	-3%	-1%
H6	391	402	-5%	-11%	-9%	-5%	-6%	-12%	-11%	-4%	-7%	-11%	-9%
H6	391	402	-4%	-9%	-9%	-4%	-5%	-10%	-12%	-3%	-7%	-10%	-8%
S1S2#	403	408	-4%	-21%	-13%	-10%	-5%	-19%	-18%	-5%	-12%	-18%	-9%
S1S2#	403	408	-7%	-20%	-13%	-5%	-9%	-17%	-17%	-5%	-12%	-17%	-12%
S1S2	403	410	-9%	-22%	-16%	-11%	-8%	-23%	-22%	-7%	-14%	-21%	-15%
H7	410	420	0%	2%	2%	0%	2%	1%	1%	0%	2%	1%	1%
H8	421	428	1%	0%	0%	-1%	-2%	0%	4%	0%	0%	-2%	1%
H8#	422	428	0%	-1%	0%	0%	0%	0%	5%	-1%	0%	-2%	1%
H8#	422	428	0%	0%	0%	0%	1%	-1%	1%	0%	1%	-2%	0%
H9	449	458	-1%	-7%	-3%	-2%	-3%	-5%	-3%	-2%	-4%	-6%	-4%
H10/LOOP	454	462	4%	11%	10%	3%	4%	12%	8%	0%	9%	8%	7%
H10#	463	486	-2%	-4%	-3%	-2%	-3%	-4%	-5%	-2%	-3%	-4%	-3%
H10#	463	486	-2%	-4%	-3%	-3%	-3%	-4%	-5%	-2%	-3%	-4%	-4%
H11#	490	507	-4%	-6%	-4%	-3%	-4%	-7%	-5%	-3%	-3%	-5%	-4%
H11#	490	507	-4%	-7%	-6%	-5%	-4%	-8%	-8%	-5%	-5%	-8%	-6%
H11#	490	509	-3%	-6%	-5%	-4%	-4%	-7%	-7%	-3%	-4%	-6%	-5%
H11#	490	509	-3%	-4%	-5%	-4%	-3%	-7%	-7%	-3%	-4%	-5%	-6%
H12#	526	540	0%	2%	-3%	1%	-3%	-3%	-3%	-1%	-1%	-2%	-2%
H12#	526	540	0%	0%	-3%	1%	-2%	-4%	-4%	-1%	-1%	-2%	-2%
H12	529	540	1%	1%	-3%	1%	-3%	-4%	-3%	-2%	-1%	-2%	-2%
H12#	541	554	0%	2%	1%	1%	-1%	-4%	1%	1%	-1%	0%	0%
H12#	541	554	0%	1%	1%	1%	2%	1%	1%	0%	1%	0%	1%
H12	542	554	-1%	2%	1%	0%	1%	5%	1%	0%	1%	0%	1%
H12	543	554	0%	2%	1%	2%	2%	1%	1%	1%	2%	2%	2%
H12	544	554	0%	1%	2%	1%	2%	1%	1%	1%	2%	2%	2%
H12	545	554	0%	0%	*	2%	2%	1%	1%	-1%	2%	*	1%
H12	547	554	1%	-3%	-1%	3%	-1%	0%	1%	1%	2%	0%	4%

≤-20%
≤-10%
<-5%
≤5%
>5%
≥10%

The residue numbers of analyzed peptides relative to the full-length protein have been tabulated. The percentage numbers listed under each compound name demonstrate the averaged difference in deuteration level of that corresponding peptide in the absence and presence of a ligand (the average calculation is based on five HDX experiments with different exchange times: 1, 30, 60, 900, and 4,200 sec). We consider only a change of deuteration level >5% to be significant based on the precision of the platform. A negative percentage represents an increase in protection to exchange in that region of the receptor in the presence of ligand, which indicates that the region has been protected when bound with ligand. #, the same peptide was detected with different charge states; *, peptide not detected.

(Fig. S1). A cluster analysis based on the deuterium incorporation differences reported in Table 2 was performed on these seven compounds (Fig. 1), and two significant features were observed. First, three major groups were classified, Groups 1–3. Group 1 consisted of compounds that afforded the least protection to exchange within the receptor–ligand complex, and this group was named "estradiol-like"; Group 2 consisted of compounds that resulted in intermediate protection to exchange in the β-sheet1/β-sheet2 region of the LBD and was named "raloxifene-like"; and Group 3 consisted of compounds that afforded the greatest protection of ERαLBD on ligand binding, and this group was named "4-hydroxytamoxifen-like." Second, regions of the ligand-binding pocket that exhibited differential protection to exchange were revealed. These regions included helix 2, the loop between helix 2 and helix 3, helix 3, helix 6, β-sheet1/β-sheet2 region, and helix 11. Interestingly, the segment 454–462 (the loop between helix 9, helix 10, and part of helix 10) showed destabilization (increase in H/D exchange kinetics) on binding of SERMs. This region of the receptor spans a portion of the ER dimerization interface.

We subsequently examined whether differential stabilization could be observed for structural changes within the same ligand chemotype. To this end, we analyzed a series of benzothiophenes that contained single-point structural modifications of raloxifene in the hinge and basic side-chain regions (Fig. S1). A discriminant analysis was developed according to the group classification from the cluster analysis described above. Based on the HDX signatures, the benzothiophenes were classified into the three groups defined above (Table 3) with LY88074 belonging to Group 1 ("estradiol-like"); LY156681 and LY117018 belonging to Group 2 ("raloxifene-like"); and LY165176 belonging to Group 3 ("4-hydroxytamoxifen-like"). The classification is based on the probability calculation derived from discriminant analysis of HDX signatures that readily distinguished these three categories.

Comparison of HDX Signatures with *in Vitro* Functional Assays and Atomic Resolution Structures. The HDX signatures for the ER ligands were compared with data from the uterine (Ishikawa) and breast (MCF-7) cell-based assays for these molecules. In MCF-7 breast cancer cells, the ICI 182780 and all SERMs are not readily distinguished from each other based on their ability to block estrogen-induced cell proliferation, i.e., these molecules are all potent inhibitors, and no agonistic activities were observed when the assay was run in agonist mode. In uterine endometrial Ishikawa cells, however, these ER ligands are readily differentiated, particularly when evaluated in the absence of E2 (agonist mode). In this context, the ER agonists E2 and DES induce a high relative stimulation (>400%) to 4-hydroxytamoxifen. The SERMs lasofoxifene, LY165176, and LY156681 are similar to 4-hydroxytamoxifen in their stimulatory profile, whereas raloxifene, LY117018, and bazedoxifene are less agonistic than 4-hydroxytamoxifen. These data generally agree with the HDX signatures for these molecules.

To examine the structural basis for the general agreement between the HDX data and the *in vitro* functional data, a comparison of HDX dynamics with the atomic structures was performed. The data from the HDX analysis (Table 2) was overlaid onto the x-ray structures of ERαLBD/estradiol (18) (Fig. 2*A*, PDB ID: 1ERE), ERαLBD/4-hydroxytamoxifen (19) (Fig. 2*B*, PDB ID: 3ERT), and ERαLBD/raloxifene (18) (Fig. 2*C*, PDB ID: 1ERR). The region demonstrating the most significant difference in the HDX profile is the β-sheet1/β-sheet2 region (amino acids 403–410) for 4-hydroxytamoxifen, which was protected by ≈20% to exchange. We investigated this specific fragment in PDB ID: 1ERE (estradiol) and PDB ID: 3ERT (4-hydroxytamoxifen) by calculating the water-accessible surface area in each. Because only exchangeable hydrogens are quantified in the HDX experiment, we chose to calculate the accessible surface area (ASA) using only the nitrogens and oxygens in this sequence. With estradiol as the ligand, the ASA for water is 108 Å^2 in this region, whereas the analogous

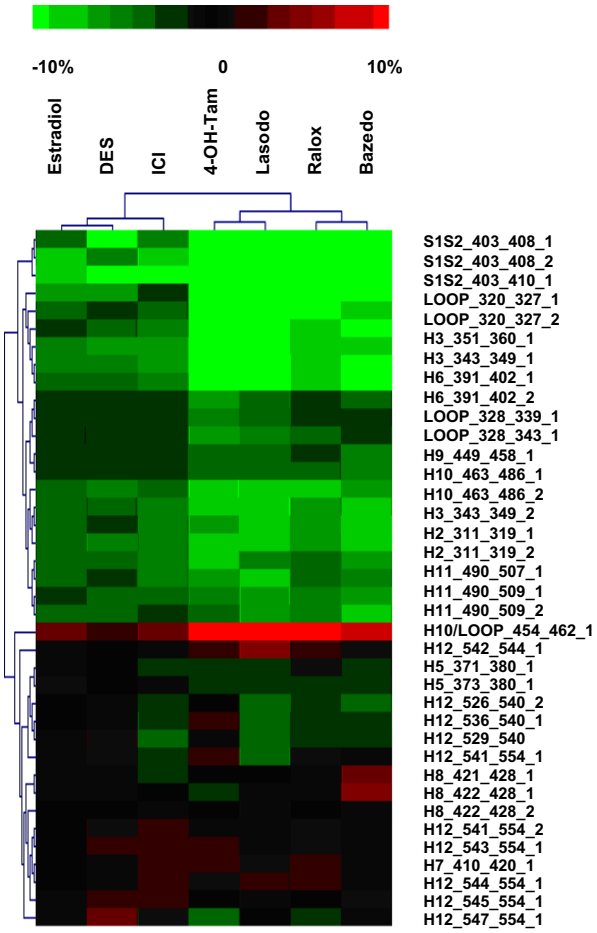

Fig. 1. Cluster analysis of known compounds. The names of the compound are shown above the bar view, and peptide regions that have been used for cluster analysis are shown on the right of the bar view. The deuterium incorporation differences of these peptides have been treated as independent variables, and each compound has been treated as a dependent variables in the cluster analysis. The color represents the differential deuterium level of each peptide in the absence and presence of the compound. The 4-hydroxytamoxifen was abbreviated as 4-OH-Tam.

surface area for 4-hydroxytamoxifen is 69 Å^2. These calculated areas are consistent with the HDX results in which lower rates of exchange are seen with 4-hydroxytamoxifen relative to estradiol, presumably because of the smaller surface area (by 39 Å^2) available for exchange when 4-hydroxytamoxifen is bound in the LBD.

Discussion

Here, we present an approach to classify ER modulators based on dynamics of the receptor–ligand complex as probed with HDX MS. To examine HDX as a tool for predicting tissue-specific functions

Table 3. Classification of unknown compounds by using discriminant analysis

Compound	Estradiol-like	4-OH-tamoxifen-like	Raloxifene-like
LY88074	1	0	0
LY156681	0	0	0.9995
LY165176	0	1	0
LY117018	0	0	1

The HDX profiles of unknown compounds are fit into the cluster-analysis model, and probability of classification is calculated. 4-OH-tamoxifen, 4-hydroxytamoxifen.

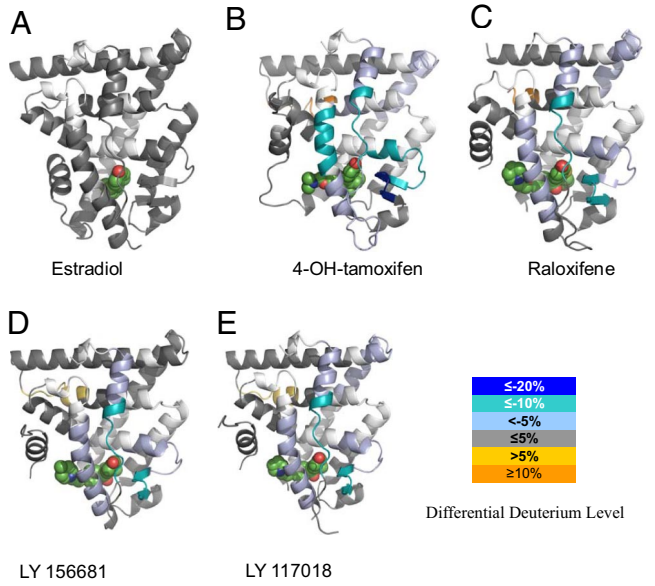

Fig. 2. ER-ligand HDX profiles. (*A–C*). HDX profile overlaid onto ER crystal structures of estradiol (PDB ID: 1ERE), 4-hydroxytamoxifen (PDB ID: 3ERT, the 4-hydroxytamoxifen was abbreviated as 4-OH-tamoxifen), and raloxifene (PDB ID: 1ERR). (*D* and *E*). HDX profile overlaid onto ER crystal structure with LY156681 and LY117018. The color legend shows the deuterium incorporation difference by subtracting deuterium incorporation content of *holo* ER from *apo* ER. The regions in the crystal structure that are colored as white belong to peptides that are not detected after pepsin digestion or cannot be measured accurately in the HDX experiments because of coelution problems.

of SERMs, we examined a spectrum of known ER modulators of diverse chemical structure with defined pharmacological profiles that ranged from full agonists to pure antagonist. We evaluated these modulators for receptor binding and their tissue-specific activity in uterine and breast cells. Ishikawa and MCF-7 cell-based assays were selected as markers of uterine and breast tissue selectivity, respectively, based on their ability to differentiate raloxifene from 4-hydroxytamoxifen. It has been demonstrated that the expression of ERα was high versus the low, or barely detectable, expression of ERβ in the ER α-positive MCF7 cells (20). ERα expression was approximately twofold greater than ERβ in the Ishikawa cells (16). In these two assays, we evaluated ER agonists (E2, DES), SERMs (raloxifene, 4-hydroxytamoxifen, lasofoxifene, bazedoxifene) and the pure antagonist ICI 182780. As expected, the agonists E2 and DES do not inhibit MCF-7 breast cancer cell proliferation, whereas the SERMs and ICI 182780 are potent inhibitors with half-maximal inhibitory concentrations of $<$10 nM (Table 1). This contrasts the effects of these ER ligands on uterine endometrial stimulation in Ishikawa cells, where 4-hydroxytamoxifen and lasofoxifene are agonists with stimulatory efficacies of 131% and 66%, respectively. In comparison, raloxifene and bazedoxifene are significantly less stimulatory to Ishikawa cells, with maximal percentage efficacies of 29% and 8%, respectively. These data are consistent with the preclinical and clinical pharmacology for tamoxifen, raloxifene, lasofoxifene, and bazedoxifene (21, 22). These results were then compared with their respective HDX signatures.

Overall, HDX signatures differentiated ER agonists and SERMs according to their uterine profiles in Ishikawa cells. For example, the potent agonists E2 and DES had similar effects in protecting the exchange of hydrogen for deuterium in ERα. The agonist HDX signature, in which little stabilization of the receptor occurs, is clearly differentiated from that of SERMs in which significant receptor stabilization is noted in helix 2, the loop between helix 2 and helix 3, helix 3, helix 6, the β-sheet1/β-sheet2 region, and helix

11. Moreover, raloxifene and 4-hydroxytamoxifen have different HDX profiles demonstrating a twofold increase in protection in the β-sheet region. Listed in Table 2, the average deuteration level of the β-sheet region in raloxifene is ≈10%, which is approximately half of that observed for 4-hydroxytamoxifen (≈20%). The HDX profile for lasofoxifene most closely resembles that of 4-hydroxytamoxifen whereas bazedoxifene is "raloxifene-like." Therefore, we have demonstrated that HDX is able to functionally discriminate ER ligands of different chemical classes in a manner consistent with the pharmacological functional profiles.

The differences in HDX profiles between 4-hydroxytamoxifen and raloxifene are intriguing. Traditionally, ER antagonism is thought to rely on the position of helix 12, which is able to disrupt the natural receptor–coactivator interaction (18, 19) (Fig. 2 *B–E*). However, the difference in the position of helix 12, when comparing crystal structures of raloxifene and 4-hydroxytamoxifen, is minimal (Fig. 2 *B* and *C*), and there is only a 1-Å difference between the basic side chain of raloxifene or 4-hydroxytamoxifen and D351 in the ERα LBD (23). In contrast to the repositioning of H12 that has been observed by protein crystallography, we observed no change to the dynamics of helix 12 on binding agonist, antagonist, or SERM molecules. In other words, although the position of helix 12 is crucial in determining the agonism versus antagonism, repositioning of helix 12 on ligand binding in the absence of coactivator does not alter the dynamics of helix 12, which exhibits rapid exchange in HDX experiments regardless of the nature of the ligand, which was surprising, given its important role in coactivator recruitment. However, these data may be complicated by the lack of the F domain (the ERαLBD used for these studies comprised residues 298–554). It can, however, be concluded that the HDX dynamics of the shorter version of helix 12 exhibit no significant stabilization on binding of ligands used in this study. It may be that stabilization of helix 12 is observed only in the presence of coactivators. Nevertheless, investigation of the ER–ligand–coactivator complex is beyond the scope of this study.

However, other regions of ERαLBD have significantly different stabilization effects on binding with 4-hydroxytamoxifen and raloxifene. The β-sheet1/β-sheet2 peptides experienced the most significant change on binding with 4-hydroxytamoxifen and raloxifene. The stabilization effect of the β-sheet region is twofold more in the 4-hydroxytamoxifen-bound complex than that in the raloxifene-bound complex. Other regions experience various degrees of stabilization and can be used in combination with the β-sheet region to discriminate 4-hydroxytamoxifen and raloxifene. Comparison of these regions to the protein crystal structure can help us to better understand the effect of SERM binding to ERα. In Fig. 2 *B* and *C*, the peptide region of the β-sheet1/β-sheet2 region experiences the most significant stabilization on binding with the 4-hydroxytamoxifen-like compound group. This region is opposite to helix 12 and is distant from the basic side chain of the SERM molecules. The calculated solvent ASA of the β-sheet1/β-sheet2 region indicates that estradiol imparts a significantly larger area of accessibility to water than does 4-hydroxytamoxifen, data that are consistent with the HDX results. Careful examination of the compound orientation in the ERαLBD ligand-binding pocket by correlating to the HDX dynamics may suggest new directions of chemical moiety modification.

In addition to binning ER ligands of unlike chemical structures, HDX was able to differentiate subtle structural changes at the molecular level within the same chemotype. This was established by evaluating a series of benzothiophene analogs (24) of raloxifene in which specific point modifications were made that altered the position or nature of basic side chain, a key pharmacophore that interacts with D351. Our analysis shows that ligand-binding modes can indeed be affected by small chemical modifications. The different binding modes are revealed by the different stabilization effects on helix 2, the loop between helix 2 and helix 3, helix 3, helix 6, the β-sheet1/β-sheet2 region, and helix 11. Moreover, HDX profiling is consistent with the observed tissue-selective pharmacological profiles for these compounds. For example, LY88074 is a raloxifene analog in which the basic side chain has been removed. This compound stimulates uterine cell proliferation. The HDX profile demonstrates stabilization most similar to that of estrogen agonists such as E2 and DES. Removing the carbonyl from the hinge region of raloxifene gives LY165176, a SERM that resembles tamoxifen in uterine agonist pharmacology both in cell culture and in rodents (24). These data are consistent with the HDX fingerprint for LY165176, which shows stabilization in the β-sheet regions similar to that of 4-hydroxytamoxifen. The benzothiophene analogs LY156681 and LY117018 (Table 2) share the same ER-binding mode as shown by HDX dynamics, an observation that is also supported by the x-ray structures (Fig. 2 *D* and *E* and Table S1). In the x-ray structures, these two compounds have almost the same orientation in the ERαLBD. LY117018 differs in structure from raloxifene by only a methylene group in the basic side chain and is pharmacologically similar to raloxifene *in vitro* (Table 1) and *in vivo*, data that are consistent with the HDX fingerprints for these molecules.

Although the findings from the HDX studies are consistent with the uterine endometrial data, there were two significant exceptions observed. ICI 182780 exhibits minimal estrogen agonism in the Ishikawa assay yet shows a similar HDX profile to that of the agonists. Although the origin of this fingerprint is not clear, the protein crystal structure of ICI 164384/ERβ (25) is unique in that the salt bridge between the ligand and helix 3, a common feature for SERMs, is not formed because of the intrinsic structural nature of the nonbasic side chain in the ICI compound. The absence of this important interaction may explain the lack of HDX protection in regions like the peptide region between helix 2 and helix 3 (LOOP), helix 3, and β-sheet1/β-sheet2 (as listed in Table 2). Conversely, the increased protection of helix 3, helix 5, and β-sheet1/β-sheet2 by SERMs may be directly related to the strong salt bridge between the SERM basic side chain and the Asp in helix 3. A similar observation for pure agonist and antagonist–receptor interactions was observed through dimer stabilization effects and fluorescence anisotropy (2, 26). In the work of Tamrazi *et al.*, the ER–ICI complex exhibited a similar degree of dimer stabilization to that of the ER–agonist complexes, all of which were reduced when compared with ER–SERM complexes. In addition, the ER–ICI complex and ER–agonist complexes showed higher anisotropy than that of ER–SERM complexes, indicating reduced regional dynamics for the helix 11 region. The similarity between ER/agonist and ER/antagonist structure dynamics probed by these other techniques correlates with our observations of reduced HDX dynamics for ER in the presence of agonists and ICI, compared with of the degree of stabilization induced after binding of SERMs. Within the benzothiophene class, LY156681 is the only analog in which the HDX profiling did not correspond to the agonist/antagonist profile observed in the Ishikawa assay, i.e., LY156681 is a potent agonist (EC_{50} = 5 nM with 164% stimulation) similar to that of 4-hydroxytamoxifen yet exhibited a HDX fingerprint more closely related to raloxifene. The origins of these differences are not clear, although small aliphatic substituents on the basic side chain in other SERM scaffolds have been postulated to destabilize the antagonist conformation of helix 12, leading to partial agonist effects (27, 28). Overall, classification of ER ligands with HDX profiling provides a more functional-based compound classification when compared with the compound classification based on chemical structures.

Although direct interactions between receptor and ligand are thought to mediate much of the tissue selectivity observed for SERMs, the *in vivo* pharmacokinetic and pharmacodynamic properties of these molecules may play a role as well. For example, the metabolism of tamoxifen is complex. This SERM undergoes metabolic oxidation to its active metabolite, 4-hydroxytamoxifen, which can further isomerize to E and Z isomers having different receptor

profiles (29, 30). Other SERMs, such as raloxifene and lasofoxifene, undergo metabolic glucuronidation (31, 32). Tissue-selective conversion of circulating metabolite to parent compound cannot be ruled out as a contributing factor to the observed pharmacology. However, categorizing SERM function from the receptor level grants simplified means to evaluate SERMs, which requires sophisticated designs to bridge structure and function studies effectively. Our work using HDX MS to characterize SERMs described here provides insight into molecular mechanism of action of these drugs and provides a superior biochemical method for predicting the tissue-specificity profile. Clearly, this technique reveals different binding modes of ER ligands and classifies ligands based on ER structural dynamics even though the compounds belong to the same chemical scaffold. Although the merit of cell-based assays to reveal drug functionalities in different cell lines cannot be overlooked, the HDX MS platform as a single biochemical assay offers the potential to replace multiple cell-based test procedures. On the other hand, HDX MS provides information beyond that which can be obtained from analysis of the x-ray crystal structures of ER with several SERMs and can differentiate the tissue-selective pharmacologies of SERMs within a biochemical assay. This approach moves the low-throughput hurdle within the x-ray structure-determination method and provides a promising function-based alternative biochemical screen. Thus, this method has enormous potential because it may be used to identify SERMs that induce favorable and/or novel receptor dynamics that may represent new generations of SERMs with improved selectivity and safety profiles.

Methods

HDX Analysis. HDX experiments were carried out with a LEAP Technologies Twin HTS PAL liquid handling robot interfaced with a Thermo Finnigan linear ion trap mass spectrometer (12). For details, see *SI Methods*.

Protein Production, ER Binding, MCF-7, and Ishikawa Assays. For details see *SI Methods*.

Statistical Analysis. Cluster analysis was performed for seven known compounds with MultiExperiment Viewer (TM4, V4.0) (33). Different cluster methods including average linkage, complete linkage, and single linkage cluster were used, and all rendered similar results. Based on the classification of three groups from the cluster analysis, we developed a discriminant analysis model, where the peptide deuterium changes were treated as independent variables, and the compounds were treated as dependent variables. The procedures StepDisc and Discrim (SRS 9.1.3 Service Pack 4) were used to perform the stepwise discriminant analysis. A stepwise selection was first used to remove the multicollinearity of the data. A total of five peptides were selected for the classification of the four benzothiophenes with discriminant analysis, where the classification function is shown in the following equation:

$$\text{Group}_i = \sum_j w_{ij}x_j + \text{constant};$$

$$i = 1, \ldots, n; \quad j = 1, \ldots, n,$$

where i corresponds to groups, and w_{ij} is the weight for the jth variable x. Variable x is the percentage numbers of the differences in deuteration level of each peptides in the HDX experiment, and selected variables and the weights for each variable were shown in Table S2. The classification of the four benzothiophenes and the probability values were derived from Fisher's linear discriminant analysis based on the selected peptides (34–36). The SAS program was developed to implement the discriminant analysis models for parameter estimation. The probability values for the benzonthiophenes to belong to different groups are reported in Table 3.

Crystallization and Data Collection. See *SI Methods* for details. The accessible surface area for PDB IDs 1ERE, 1ERR, and 3ERT were calculated with AREAIMOL in CCP4 4.0 with water as probe (radius of 1.4 Å). No protein treatment before the calculation. The B-factor column of the PDB file was replaced by the ASA for each atom. The sums of the residues of interests were calculated as ASA for the region (37).

ACKNOWLEDGMENTS. This work was supported, in part, by the state of Florida. The efforts of P.R.G. were supported by National Institutes of Health Molecular Library Screening Center Network Grant U54MH074404 (to H. Rosen, Principal Investigator).

1. McDonnell DP (2006) Mechanism-based discovery as an approach to identify the next generation of estrogen receptor modulators. *FASEB J* 20:2432–2434.
2. Tamrazi A, Carlson KE, Katzenellenbogen JA (2003) Molecular sensors of estrogen receptor conformations and dynamics. *Mol Endocrinol* 17:2593–2602.
3. Tamrazi A, Katzenellenbogen JA (2003) Site-specific fluorescent labeling of estrogen receptors and structure–activity relationships of ligands in terms of receptor dimer stability. *Methods Enzymol* 364:37–53.
4. Tamrazi A, Carlson KE, Rodriguez AL, Katzenellenbogen JA (2005) Coactivator proteins as determinants of estrogen receptor structure and function: Spectroscopic evidence for a novel coactivator-stabilized receptor conformation. *Mol Endocrinol* 19:1516–1528.
5. Yan X, Broderick D, Leid ME, Schimerlik MI, Deinzer ML (2004) Dynamics and ligand-induced solvent accessibility changes in human retinoid X receptor homodimer determined by hydrogen deuterium exchange and mass spectrometry. *Biochemistry* 43:909–917.
6. Wales TE, Engen JR (2006) Hydrogen exchange mass spectrometry for the analysis of protein dynamics. *Mass Spectrom Rev* 25:158–170.
7. Quint P, *et al.* (2006) Structural mobility in human manganese superoxide dismutase. *Biochemistry* 45:8209–8215.
8. Mandell JG, Falick AM, Komives EA (1998) Identification of protein–protein interfaces by decreased amide proton solvent accessibility. *Proc Natl Acad Sci USA* 95:14705–14710.
9. Hamuro Y, *et al.* (2003) Dynamics of cAPK type IIbeta activation revealed by enhanced amide H/2H exchange mass spectrometry (DXMS). *J Mol Biol* 327:1065–1076.
10. Hamuro Y, *et al.* (2003) Rapid analysis of protein structure and dynamics by hydrogen/deuterium exchange mass spectrometry. *J Biomol Tech* 14:171–182.
11. Englander JJ, *et al.* (2003) Protein structure change studied by hydrogen–deuterium exchange, functional labeling, and mass spectrometry. *Proc Natl Acad Sci USA* 100:7057–7062.
12. Chalmers MJ, *et al.* (2006) Probing protein ligand interactions by automated hydrogen/deuterium exchange mass spectrometry. *Anal Chem* 78:1005–1014.
13. Bruning JB, *et al.* (2007) Partial agonists activate PPARg using a helix 12 independent mechanism. *Structure (London)* 15:1–14.
14. Englander SW (2006) Hydrogen exchange and mass spectrometry: A historical perspective. *J Am Soc Mass Spectrom* 17:1481–1489.
15. Yan X, *et al.* (2006) Investigation of ligand interactions with human RXRalpha by hydrogen/deuterium exchange and mass spectrometry. *J Am Soc Mass Spectrom* 17:1510–1517.
16. Bramlett KS, Burris TP (2003) Target specificity of selective estrogen receptor modulators within human endometrial cancer cells. *J Steroid Biochem Mol Biol* 86:27–34.
17. Borgna JL, Rochefort H (1980) High-affinity binding to the estrogen receptor of [3H]4-hydroxytamoxifen, an active antiestrogen metabolite. *Mol Cell Endocrinol* 20:71–85.
18. Brzozowski AM, *et al.* (1997) Molecular basis of agonism and antagonism in the oestrogen receptor. *Nature* 389:753–758.
19. Shiau AK, *et al.* (1998) The structural basis of estrogen receptor/coactivator recognition and the antagonism of this interaction by tamoxifen. *Cell* 95:927–937.
20. Chang EC, Frasor J, Komm B, Katzenellenbogen BS (2006) Impact of estrogen receptor beta on gene networks regulated by estrogen receptor alpha in breast cancer cells. *Endocrinology* 147:4831–4842.
21. Komm BS, *et al.* (2005) Bazedoxifene acetate: A selective estrogen receptor modulator with improved selectivity. *Endocrinology* 146:3999–4008.
22. Ke, HZ, *et al.* (1998) Effects of CP-336,156, a new, nonsteroidal estrogen agonist/antagonist, on bone, serum cholesterol, uterus and body composition in rat models. *Endocrinology* 139:2068–2076.
23. Jordan VC (2003) Antiestrogens and selective estrogen receptor modulators as multifunctional medicines. 1. Receptor interactions. *J Med Chem* 46:883–908.
24. Grese TA, *et al.* (1997) Molecular determinants of tissue selectivity in estrogen receptor modulators. *Proc Natl Acad Sci USA* 94:14105–14110.
25. Pike AC, *et al.*(2001) Structural insights into the mode of action of a pure antiestrogen. *Structure (London)* 9:145–153.
26. Tamrazi A, Carlson KE, Daniels JR, Hurth KM, Katzenellenbogen JA (2002) Estrogen receptor dimerization: ligand binding regulates dimer affinity and dimer dissociation rate. *Mol Endocrinol* 16:2706–2719.
27. Blizzard TA, *et al.* (2004) Estrogen receptor ligands. Part 8: Dihydrobenzoxathiin SERAMs with heteroatom-substituted side chains. *Bioorg Med Chem Lett* 14:3865–3868.
28. Blizzard, *et al.* (2004) Estrogen receptor ligands. Part 7: Dihydrobenzoxathiin SERAMs with bicyclic amine side chains. *Bioorg Med Chem Lett* 14:3861–3864.
29. Katzenellenbogen JA, Carlson KE, Katzenellenbogen BS (1985) Facile geometric isomerization of phenolic non-steroidal estrogens and antiestrogens: Limitations to the interpretation of experiments characterizing the activity of individual isomers. *J Steroid Biochem* 22:589–596.
30. Jordan VC, Collins MM, Rowsby L, Prestwich G (1977) A monohydroxylated metabolite of tamoxifen with potent antioestrogenic activity. *J Endocrinol* 75:305–316.
31. Rosati RL, *et al.* (1998) Discovery and preclinical pharmacology of a novel, potent, nonsteroidal estrogen receptor agonist/antagonist, CP-336156, a diaryltetrahydronaphthalene. *J Med Chem* 41:2928–2931.
32. Lindstrom TD, Whitaker NG, Whitaker GW (1984) Disposition and metabolism of a new benzothiophene antiestrogen in rats, dogs and monkeys. *Xenobiotica Fate Foreign Compounds Biol Syst* 14:841–847.
33. Saeed AI, *et al.* (2003) TM4: A free, open-source system for microarray data management and analysis. *BioTechniques* 34:374–378.
34. Morrison, DF (1976) *Multivariate Statistical Methods* (McGraw–Hill, New York).
35. Mendez MA, Hodar C, Vulpe C, Gonzalez M, Cambiazo V (2002) Discriminant analysis to evaluate clustering of gene expression data. *FEBS Lett* 522:24–28.
36. Dudoit S, Fridlyand J, Speed TP (2002) Comparison of discrimination methods for the classification of tumors using gene expression data. *J Am Stat Assoc* 97:77–87.
37. Shrake A, Rupley JA (1973) Environment and exposure to solvent of protein atoms. Lysozyme and insulin. *J Mol Biol* 79:351–371.
38. Geiser AG, *et al.* (2005) A new selective estrogen receptor modulator with potent uterine antagonist activity, agonist activity in bone, and minimal ovarian stimulation. *Endocrinology* 146:4524–4535.